(Preprint) AAS 10-256

AUTONOMOUS GNC FOR DESCENT AND LANDING ON SMALL, IRREGULAR BODIES

Jesus Gil-Fernandez* and Mariella Graziano †

Future missions to asteroids demand soft, pinpoint landing (few meters dispersion). The GNC system during descent and landing is autonomous, mainly constrained by cost and technological maturity, and must be robust to large uncertainties (asteroid characteristics). The selected sensors provide the necessary observables and the navigation process them to provide reliable estimates of the spacecraft complete state (absolute and surface-relative navigation). A safe descent profile is defined by a set of waypoints and corresponding timing. Guidance generates the reference maneuvers and trajectory and control computes small actions to cancel current deviations. Monte Carlo simulations prove that GNC performances meet the requirements.

INTRODUCTION

The sample return missions to small bodies, in particular near Earth asteroids, are gaining momentum within several space agencies. After the success of the Hayabusa mission, ESA's Marco Polo mission[1] aims to characterize in detail a small asteroid (lower than 1 km) and bring back to Earth an amount of asteroid soil that allows performing significant science. In addition to the basic science objectives, the asteroid data gathered in such missions will be crucial for the analysis and design of mitigation missions in case of real threat to the Earth.

One of the most critical phases during the proximity operations is the descent and landing (D&L). For the small target asteroids, the tight mission requirements, the environment uncertainties and the programmatic constraints pose very demanding challenges on the GNC system[2]. For instance, in Marco Polo mission the required landing accuracy is 3.5 m (3σ), the lowest ever for a spacecraft (SC) landing in a celestial body[3] (one order of magnitude lower than the 30 m of Hayabusa[4]).

Apart from the landing requirement, other problems drive the GNC design during the D&L operations. The main issue is that ground operators cannot be in the loop below a certain distance because the light time is too long. There is a limit altitude (low gate) from where the D&L operations will be autonomous. This altitude depends on the propellant expenditure, power and thermal systems, and visibility and illumination limits on the D&L duration.

---

* Study Manager and Technical Consultant, Advanced Space Systems & Technologies Unit, Isaac Newton 11, Tres Cantos, 28760 Madrid (Spain), Senior AIAA Member.
† Head of Advanced Space Systems & Technologies Business Unit, Isaac Newton 11, Tres Cantos, 28760 Madrid (Spain).

For autonomous operations there are factors that have a stronger impact in the GNC design than in ground controlled D&L. The asteroid characteristics at short distances might be known with significant uncertainties, for instance the local gravity field or the surface properties. Specific local characterization and rehearsal will mitigate these uncertainties but the GNC design must be robust to cope with certain level of dynamics mismodeling.

Some programmatic issues must be considered in the autonomous GNC system design. For the mission to be considered for actual implementation in the near future, the technologies used in the GNC system must currently have a sufficiently high Technology Readiness Level (TRL). As this mission will be the first of its kind for ESA some of the critical sensors and GNC technologies are not mature enough. The selected GNC technologies must place a moderate risk for the mission development. Finally, the overall cost cannot forbid the implementation as a medium-class mission. Thus, the sensor set and the technology development are tightly constrained.

There is a favorable environmental condition for the GNC design; the low dynamics allows high control authority with standard thrusters. The slow dynamics characteristic time and the control authority provide large flexibility for the design of the D&L strategy and the GNC design.

PROBLEM STATEMENT

The main objective of the GNC in D&L mode is to achieve a safe, soft, pinpoint landing[3]. The key requirements are the touch-down conditions summarized below.

1)Landing accuracy 3.5 m (3σ),

2) Horizontal velocity lower than 5 cm/s,

3) Vertical velocity lower than 30 cm/s, and

4) Misalignment of the SC wrt the surface lower than 10º.

As it was mentioned above, the GNC must be fully autonomous below the low gate because the communications delay (~20 minutes) is longer than the total D&L duration. The D&L duration was mainly limited by illumination constraints, battery sizing, and delta-V budget. It is important to note the hazard avoidance is not required because the landing site is fully characterized before the D&L (low altitude hovering, D&L rehearsals). At the low gate, the ground control gives the GO command and the autonomous operations starts. The low gate is placed in a safe location that ensures landing site visibility and is within the operational range of the descent altimeter.

The D&L trajectory must be defined fulfilling several mission and system constraints. Taking advantage of the weak dynamics environment and high control authority, the descent profile is defined by a set of waypoints and associated times. These times define the descent rate or the station keeping duration. The waypoints are defined by the ground control before the start of the close D&L and must fulfill the safety constraints (avoid collision with the surface of the irregular asteroid) and system constraints (e.g. image processing limits on the angular velocity). The waypoint-based strategy provides a high flexibility in the definition of the descent profile in order to adapt to any asteroid shape and operational constraints.

The selection of the sensors is part of the GNC design. Many sensor set options have been traded in order to achieve the required observables for the navigation. With the considered mission and system constraints, the preferred sensor suite is listed below.

1) Two redundant laser altimeters used at distances larger than the low gate altitude (~100 m), the proximity operations not part of the D&L

2) One ‘nadir-pointing’ miniature radar altimeter (MRA) for distances below the low gate.

3) Three MRA surrounding the ‘nadir-poiting’ one, tilted to measure the surface-relative attitude (and provide redundant altitude measurements).

4) Two redundant ‘nadir-pointing’ wide angle cameras (WAC) for absolute and relative navigation.

5) Two redundant, top-mounted, tilted WAC for contingency and surface operations.

6) Three redundant STR for attitude determination and vision-based navigation during the approach phase (from target detection and identification starting at ~300.000 km to far station keeping at 20 km).

7) Two redundant IMU.

The actuators consist of a set of thrusters providing force and torque in any direction with no need of rotations (not to jeopardize the feature tracking carried out by the image processing function and to reduce the size of the reaction wheels), and 4 reaction wheels to compensate attitude disturbances.

The reference scenario for the validation of the GNC system is depicted in topocentric frame in Fig.1. It includes several hold points (hovering) for sensor acquisition, navigation switch or navigation convergence before the final burn for landing.

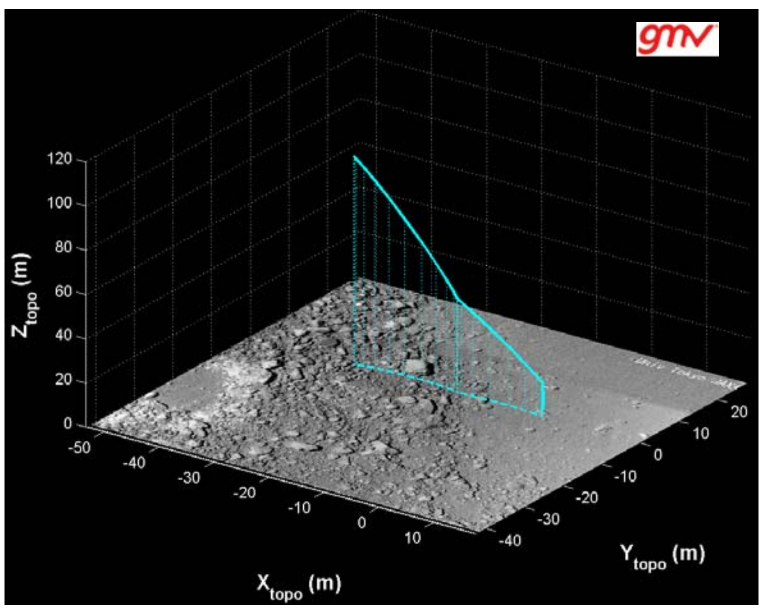

Figure 1. Close descent trajectory in topocentric frame (benchmark scenario).

AUTONOMOUS GNC ALGORITHMS

Navigation

The navigation function must be able to filter the range measurements from the different altimeters and the output of the image processing function, either line-of-sight (LOS) to known landmarks for absolute navigation or unknown landmarks for relative navigation. Thus, the dimension of the measurement vector changes from epoch to epoch. For instance, the landmarks disappear from the FOV of the camera while the altitude decreases, and the tilted MRA are activated at 50 m and only provide range observations below that altitude.

The augmented state vector includes the SC state with respect to the asteroid centre of mass, and some considered parameters from the dynamics and observables models. These considered parameters prevent the filter divergence without inclusion of artificial noise. The components of the state vector changes when the landmarks appear or disappear from the measurement vector. This variation must be properly addressed in the a priori covariance matrix construction.

The navigation function is implemented by an unscented Kalman filter (UKF)[5]. Compared to an extended Kalman filter, the UKF provides two main advantages,

1) Higher-order approximation (up to 3rd-order in some cases) to the statistics of non-linear measurements and parameters, and

2) No need to derive the partial equations for the measurements and dynamics, thus allows a faster implementation of new measurements or components of the state vector.

For the unscented transformation we consider (2N+1) sigma points, 2N points from the square root of the covariance matrix and the mean state, as presented in Eq. (1). With these sigma points, the covariance propagation requires the same number of propagations than the EKF if numerical central differences are used to compute the transition matrix.

$$
\begin{aligned}
\hat{x}_{k-1}^{(0)} &= \hat{x}_{k-1}^{+} & & \\
\hat{x}_{k-1}^{(i)} &= \hat{x}_{k-1}^{+} + \tilde{x}^{(i)} & & i = 1,\ldots,2n \\
\tilde{x}^{(i)} &= \left(\sqrt{(n+\kappa)P_{k-1}^{+}}\right)_i^T & & i = 1,\ldots,n \\
\tilde{x}^{(n+i)} &= -\left(\sqrt{(n+\kappa)P_{k-1}^{+}}\right)_i^T & & i = 1,\ldots,n
\end{aligned}
\tag{1}
$$

The time update of the SC state is implemented with an analytical propagation, the same propagation implemented in the guidance and control algorithms. This analytical integration of the equation of motion provides a closed-form solution of the a priori state at the time of measurement from the a posteriori state vector at the previous measurement time. A fixed-step, 4th-order Runge-Kutta numerical integration scheme is quite efficient and was also implemented for comparison. The analytical propagation is as accurate as the numerical propagation and is almost one order of magnitude faster than the numerical propagation.

Guidance

The guidance function shall compute the reference thrust profile that brings the SC from the current state to the next waypoint at the prescribed time. Thus, the guidance algorithm must compute the thrust profile that achieves a fixed-time transfer with specified initial and final conditions, minimizing the propellant expenditure and fulfilling the operational constraints. Two types of guidance algorithms are implemented[6], their use depends on the thrust level available, one is intended for impulsive maneuvers and the other for low-thrust.

An analytical propagation scheme was developed in order to provide fast, accurate computation of the influence matrices required by the guidance and control. The discretization of the dynamics follows the model presented by Carson and Acikmese[7]. The time interval between waypoints is divided in equal duration segments. In each segment, the gravity field is approximated by a linear expansion and the zero-order hold approach is used for the control acceleration. The angular velocity of the asteroid is assumed constant (very realistic assumption during the time of the D&L). With this model the dynamics is formulated as a piece-wise Linear Time Invariant (LTI) system give in Eq.(2).

$$\dot{\vec{x}}_K = A_K \vec{x}_K + B(\tilde{g}_K + \vec{u}_K) \tag{2}$$

The dynamics can be integrated analytically and the state vector at any time can be known through the transition and input-influence matrices (calculated analytically for a given initial position and control) as given in Eq.(3), where $\{u_k\}_{1,N}$ is the column vector resulting from the concatenation of vectors from index 1 to index N, and is $:\prod_{K=0}^{N-1} f_K :$ the time-ordered product (older function placed at the right)

$$\vec{x}_N = \underbrace{:\prod_{K=0}^{N-1} \Phi(A_K; t_{K+1} - t_K):}_{\Phi_{N,0}} \vec{x}_0 + \Psi_{N,0}\{\tilde{g}_K + \vec{u}_K\}_{K=0,N-1} \tag{3}$$

The impulsive guidance algorithm is based on the differential guidance[8], taking advantage of the analytical transition matrix. The method considers instantaneous velocity changes, therefore Eq. (2) still holds but there is no control acceleration. The only control variables are the initial impulse ΔV_1 to achieve the final position and the final impulse ΔV_2 to achieve the final velocity. Equation (4) defines a determined system and can be solved explicitly.

$$\begin{Bmatrix} \vec{r}_N \\ \vec{v}_N \end{Bmatrix} = \Phi_{N,0} \begin{Bmatrix} \vec{r}_0 \\ \vec{v}_0 + \Delta V_1 \end{Bmatrix} + \begin{Bmatrix} 0 \\ \Delta V_2 \end{Bmatrix} \tag{4}$$

The low-thrust guidance solves the fixed-time transfer with a direct method that shows wide radius of convergence due to the great control authority. The cost function is the sum of squares of the control acceleration (there are independent thrusters in each direction) and the trajectory design problem becomes a constrained parameter optimization problem. The initial guess is the translation into a finite burn of the impulsive problem, presented above. The optimization step is analytically solved as given in Eq.(5), where $\Delta\vec{x}_N$ is the deviation between the desired final waypoint and the propagated final SC state. The optimization solver is simple and fast enough to be implemented on-board, only few iterations are needed to smooth non-linearities not included in the optimization problem solution.

$$\delta\{\vec{u}_K\} = \Psi_{N,0}{}^T \left(\Psi_{N,0}\Psi_{N,0}{}^T\right)^{-1} \Delta\vec{x}_N \tag{5}$$

Control

For safety reasons the reference descent trajectory must be accurately followed and the control function shall compute small corrections to the thrust profile to cancel the deviations from the reference trajectory. The impulsive descent is controlled with discrete impulses executed (if needed) at predefined times. The control algorithm is basically the same guidance algorithm but applied at intermediate times. In the control case, the delta-V are called trajectory corrective maneuvers (TCM) as depicted in Fig. 2. Only one TCM between hold points is necessary for the reference D&L scenario.

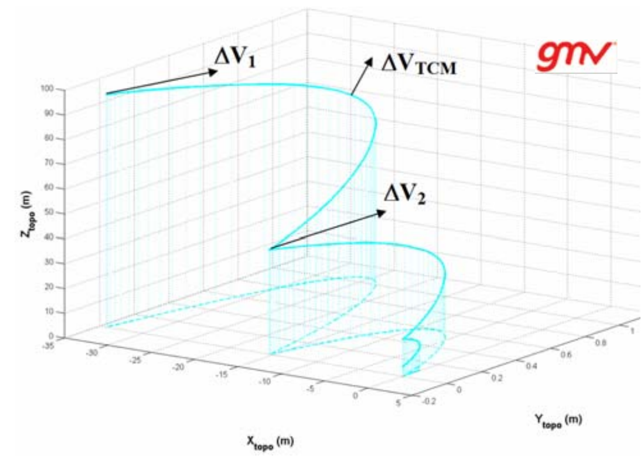

Figure 2. Differential guidance scheme for trajectory guidance and control with high-thrust

The design of the low-thrust control is based on solving a finite-horizon optimal control[9] problem presented in Eq. (6).This problem is similar to the guidance problem, but in the control the cost function is the sum of squares of the corrections to the nominal control acceleration. A closed-form solution of the improving steps for the control corrections is found taking advantage of the analytical dynamics propagation (see Ref. 6). The algorithm can be applied to a fixed horizon or a receding horizon problem because of the high control authority that prevents saturation.

$$\min_{\delta\{\vec{u}_K\}} J = \sum_{K=0}^{N-1} \left\| \delta\vec{u}_K \right\|^2 \quad \text{, subject to}$$

$$\begin{cases} \dot{\vec{x}}_K = A_K \vec{x}_K + B(\tilde{g}_K + \vec{u}_K), \ \forall k = 0,..., N-1 \\ \vec{x}_N = \vec{x}_F \\ u_{K,i} \in [-a_{K\max}, a_{K\max}], \ \ \forall i = 1,...,3 \ , \forall k = 0,..., N-1, \ \ \text{where } a_{K\max} = -T_{\max} / m_K \end{cases} \tag{6}$$

In addition, a hovering control mode shall cancel the deviation with respect to the reference hold point. For this station keeping mode, an optimal state feedback control has been implemented. The feedback gain is computed on ground with the LQR method and uploaded along with the D&L operations table. Non-linear effects (saturation, minimum impulse bit) are included at the end of all the control commanded accelerations.

PERFORMANCE ASSESSMENT

The GNC system was tested in closed-loop in a mission performance simulator. The descent profile for the benchmark scenario is depicted in Fig. 1. The SC mass is 1000 kg and 10-N thrusters were selected. The selected asteroid is 1999 JU3 that currently presents some uncertainty in its characteristics. The worst case for the landing accuracy is considered, the average diameter is 1080 m and the mass is 9.89e11 kg. This scenario is envisaged to prove the capabilities of the GNC in non benign conditions.

The navigation results of one realization in the nominal scenario are presented in Fig. 3. The thruster execution error (5%) disturbs the filter accuracy after each maneuver but the transient is quite short. The impact of losing the landmarks from the field of view can be appreciated. After the final burn the performances the horizontal plane diverges because there are no landmarks in view, only the altimeter is providing information of the altitude (Z-axis).

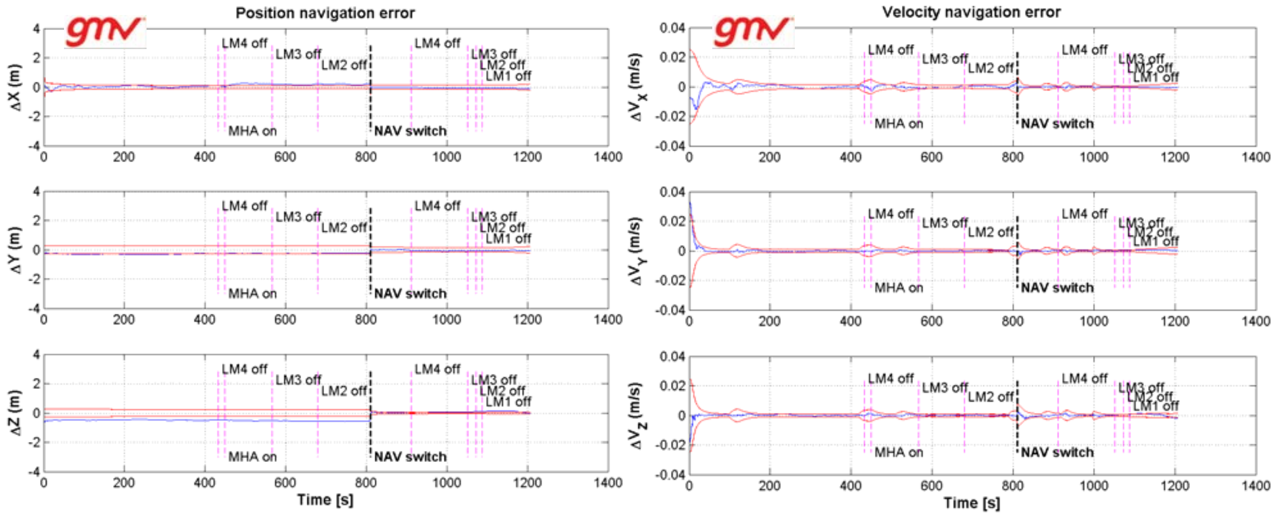

Figure 3. Position (left) and velocity (right) navigation error. Blue is actual error, red is ±1 sigma estimate. The main events in the navigation chain are indicated, landmark disappearance, navigation switch.

Monte Carlo simulations were run varying the uncertain parameters to support the system design. The parameters that have the highest impact on the landing performances are the uncertainties in the gravity field and the surface properties (mainly roughness), the image processing performances, the thruster execution error, and the attitude control system performances. The results of a Monte Carlo simulations using impulsive guidance with 10-N thrusters and control and using continuous control with 1-N thrusters are presented in Fig. 4. It follows that the continuous thrust provides higher robustness than the discrete control provided by the TCM. However, the 10-N thrusters fulfill the landing requirements and were selected for system design reasons.

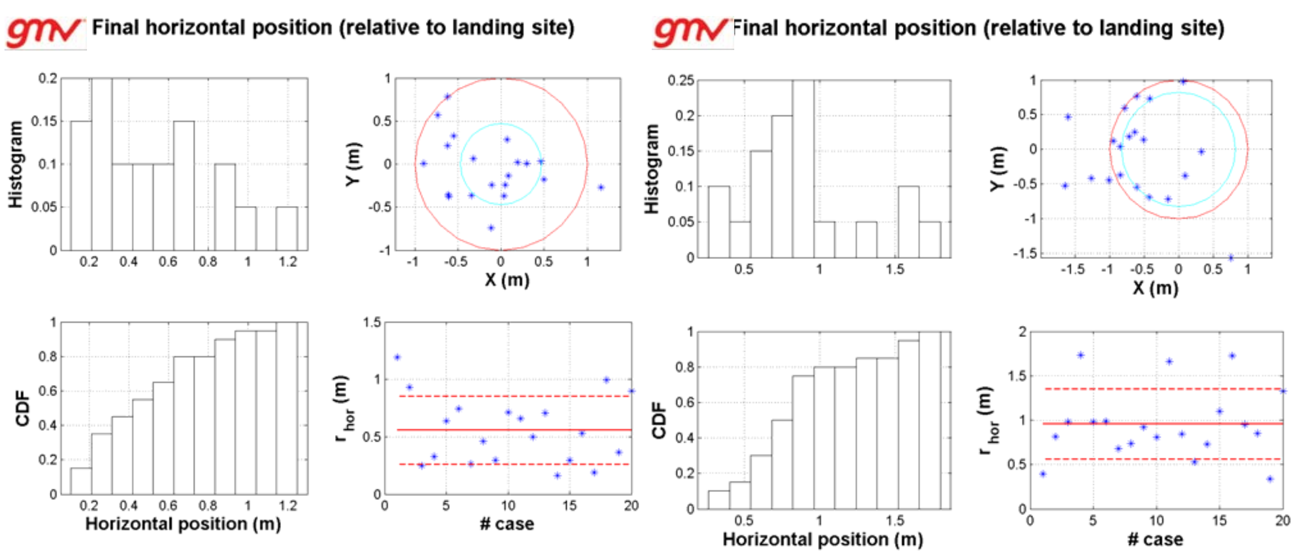

Figure 4. Landing performances for thruster selection. Left: continuous thrust (1 N). Right: impulsive (10 N)

Additional Monte Carlo simulations were carried out to test the robustness of the GNC and for sensitivity analysis of mission and system parameters. For instance, a parametric analysis has been conducted in the altitude of the last descent maneuver. The descent profile was modified accordingly to maintain the averaged descent velocity in the last 2 vertical descents. The results of this analysis are presented in Fig. 5. Each point represents the results of a Monte Carlo simulation changing the final-burn altitude. The delta-V and landing accuracy remains constant. The worst values of vertical and horizontal velocity are far below the requirements.

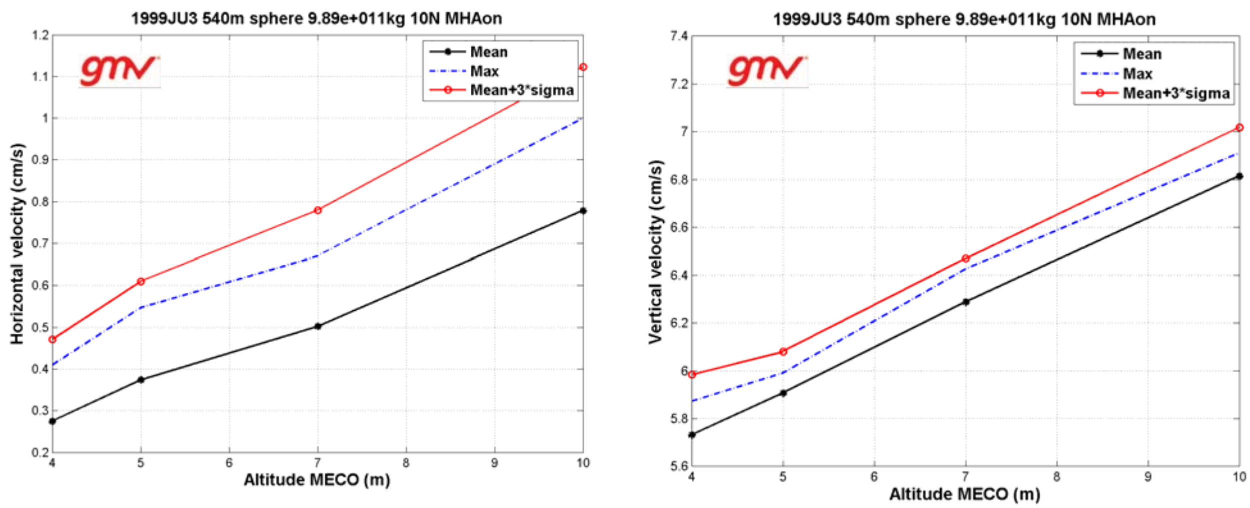

Figure 5. Parametric analysis of altitude of final burn in nominal conditions.

It might be required to land in a large, featureless region where there are no landmarks to track (hazard-free region). In order to assess the impact of the final-burn altitude on the landing performances, a parametric analysis was carried out considering no unknown landmarks below the navigation switch altitude. The results are presented in Fig. 6. In this scenario, there is a significant degradation in the landing accuracy and horizontal velocity compared to Fig.5, but still below requirements. There is a negligible impact in the vertical velocity and ΔV budget. The landing accuracy loses its meaning in a large safe region, thus the most important landing performances are the landing velocity components, which are still below the limits.

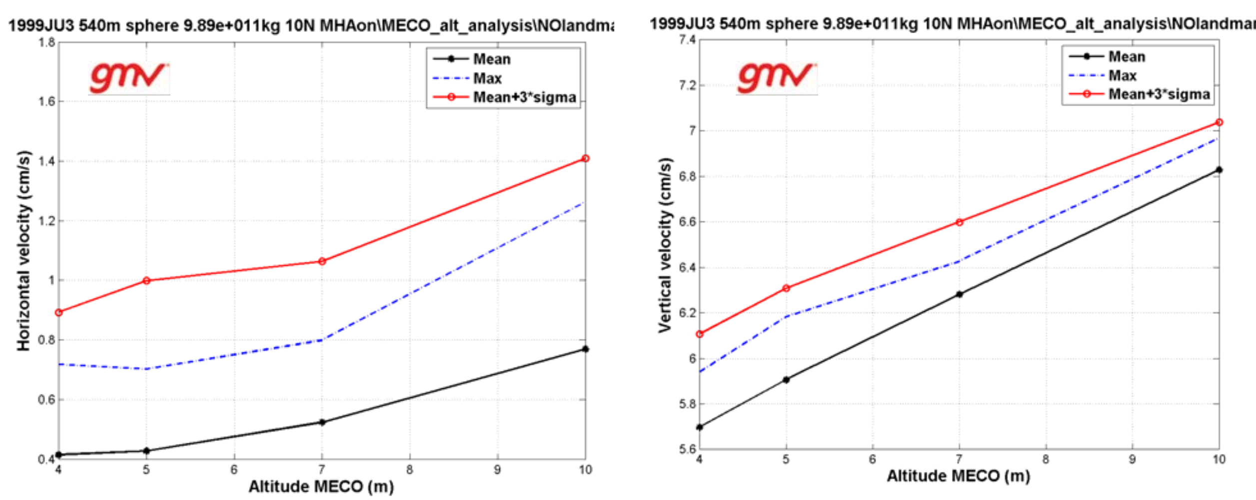

Figure 6. Parametric analysis of altitude of final burn with no unknown landmarks.

The landing performances in the finally selected nominal conditions are depicted in Fig. 7. These performances are slightly worse than those of previous figures because of higher uncertainties in the gravity field, surface normal, thruster execution errors and image processing performances. After a slight tuning of the GNC parameters and descent profile, the performances are met with enough margins.

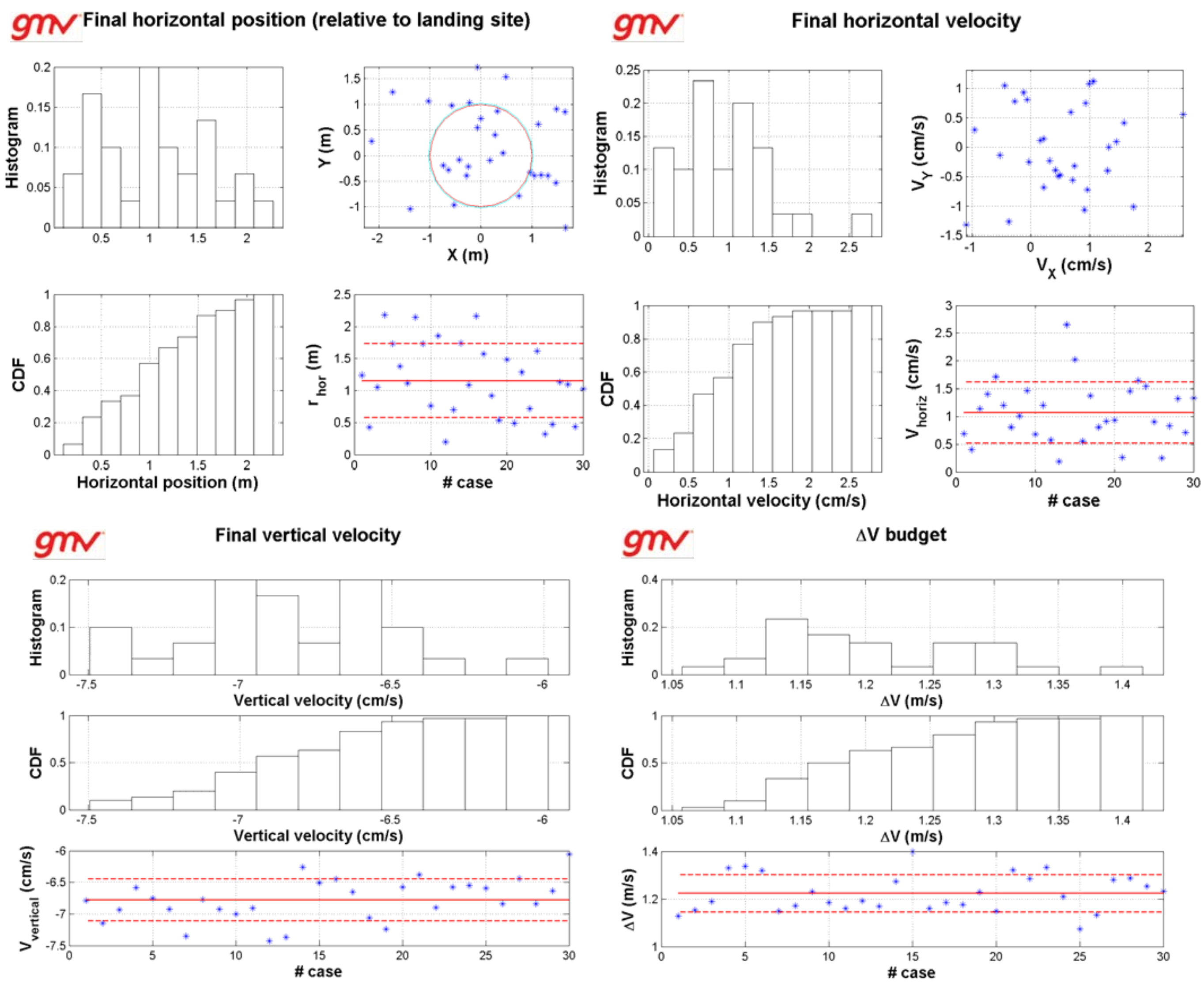

Figure 7. Landing performances for nominal scenario.

CONCLUSIONS

A GNC system to fulfill the very demanding requirements of an asteroid sample return mission has been presented. Novel GNC algorithms have been developed to satisfy the soft, pinpoint landing conditions. The GNC/AOCS system is built on European technologies with the required

TRL. The GNC system is tested in a mission performance simulator through Monte Carlo analysis. The landing performances in nominal conditions are within the mission requirements as shown in Table 1. Monte-Carlo based parametric analyses were conducted to support the mission and system design and to test the robustness of the GNC system to uncertain dynamics parameters and contingencies (thruster degradation, increased thrust execution error, lost of landmarks). For instance, under variation of the altitude of the last burn (the higher the better to avoid sample contamination with thruster exhaust products), the analysis shows that the current GNC design is robust in the absence of unknown landmarks. These results are very promising to start the development of the GNC system to reach a higher TRL.

Table 1. Nominal landing performances in reference scenario.

Magnitude	Mean	Mean+3σ	Maximum	Requirement
Landing accuracy, m	1.15	2.89	2.17	3.5 (3σ)
Horizontal velocity, cm/s	1.07	2.72	2.66	< 5
Vertical velocity, cm/s	6.78	7.77	7.42	< 30
Delta-V, m/s	1.22	1.46	1.40	-

REFERENCES

[1] *Marco Polo: Near-Earth asteroid sample return mission. Assessment Study Report*. ESA/SRE(2009)3, December 2009

[2] *M-Class Internal Review Report. Marco Polo. Technical and Programmatic Report*. SRE-PA/2009.069/Marco-Polo, 30 Oct 2009

[3] Agnolon, D., Marco Polo Mission Requirements Document, Issue 4, SCI-PA/2008. 001/Marco-Polo, 2009

[4] Jun'ichiro Kawaguchi, Shinji Hagino and Takeshi Ohshima, "Guidance And Navigation Operation For Rehearsals And Touch-Downs In Hayabusa", AAS 06-183, AAS/AIAA Space Flight Mechanics Meeting 2006, Tampa, Florida

[5] Simon, D., Optimal State Estimation, Wiley-Interscience, Hoboken, New Jersey, 2006, Chap. 14.

[6] Gil-Fernandez, J., Corral, C. "Optimal Design and Tracking of Descent and Landing Trajectories on Small, Irregular Bodies", 3rd European Conference for Aero-Space Sciences EUCASS, July 6-9th 2009, Versailles, Paris

[7] Carson, J.M., and Acikmese, A.B., "Small body GN&C research report: A guidance and control technique for small-body proximity operations with guaranteed guidance resolvability and required thruster silent time", JPL Document D-32948, Clearance #05-2804, Jet Propulsion Laboratory, California Institute of Technology, September 2005.

[8] Battin, R. H., Astronautical guidance, McGraw-Hill, 1964

[9] Carson, J.M., and Acikmese, A.B., "Small body GN&C research report: A guidance and control technique for small-body proximity operations with guaranteed guidance resolvability and required thruster silent time", JPL Document D-32948, Clearance #05-2804, Jet Propulsion Laboratory, California Institute of Technology, September 2005.